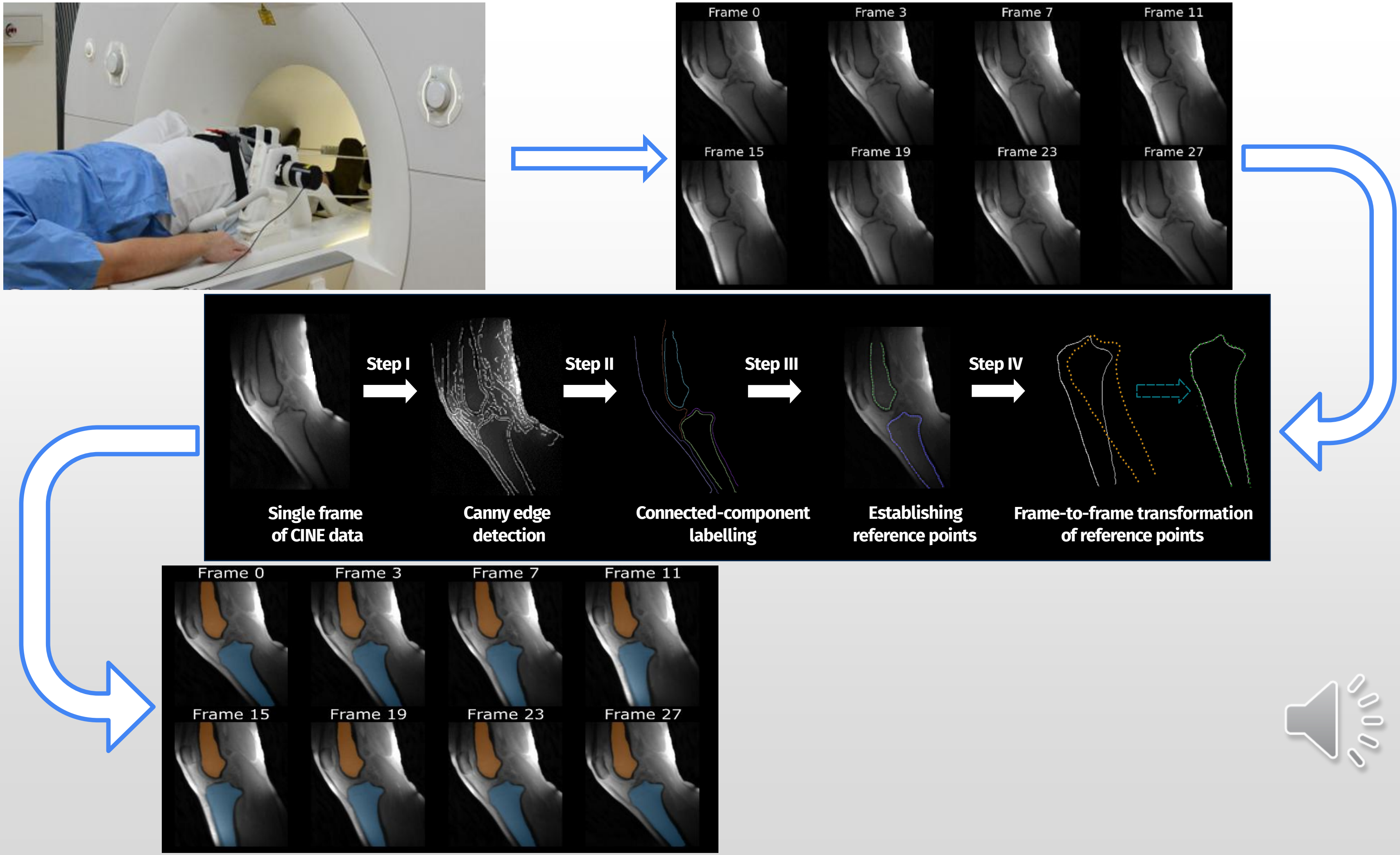
Frame 0
Frame 3
Frame 7
Frame 11
Frame 15
Frame 19
Frame 23
Frame 27
Step I
Step II
Step III
Step IV
Single frame
of CINE data
Canny edge
detection
Connected-component
labelling
Establishing
reference points
Frame-to-frame transformation
of reference points
Frame 0
Frame 3
Frame 7
Frame 11
Frame 15
Frame 19
Frame 23
Frame 27

Motivation

- Accurate assessment of osteokinematics is crucial for:
  - Evaluating joint function
  - Improving prosthetic design
  - Clinical diagnosis of knee pathologies
  - Rehabilitation monitoring

- Dynamic MRI can visualize knee motion but typically require:
  - Time-consuming manual segmentation
  - Complex registration methods
  - High-resolution static reference scans

Knee Kinematics & Pathology

- **Knee osteokinematics**: The motion of bones as rigid bodies around the knee joint
- **Bidirectional relationships**: Altered kinematics can both cause and result from joint pathologies
- **Dynamic MRI** techniques enable visualization of in vivo knee motion
- **Tracking Challenges:**
  - Need for separate high-resolution reference scans
  - Reliance on discrete landmarks
  - Time-intensive manual segmentation

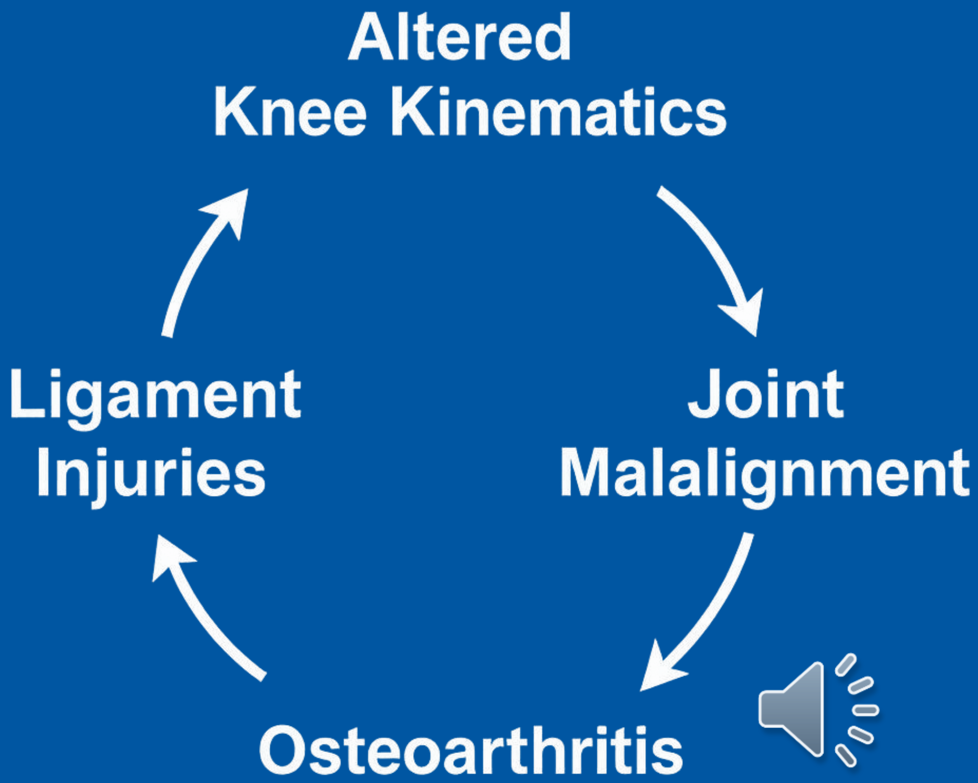

Goal: Semi-Automated Bone Tracking

Primary Objective

- Develop and validate a semi-automated pipeline to track tibiofemoral motion from sagittal plane CINE MRI
- Extract kinematic parameters during knee flexion-extension

Current Challenges

- Manual segmentation is time-consuming
- High-resolution reference scans add complexity

Expected Outcomes

- Reduced processing time
- Improved measurement consistency
- Direct analysis without additional reference scans

UNIVERSITÄTSKLINIKUM jena

MRI-compatible knee motion device

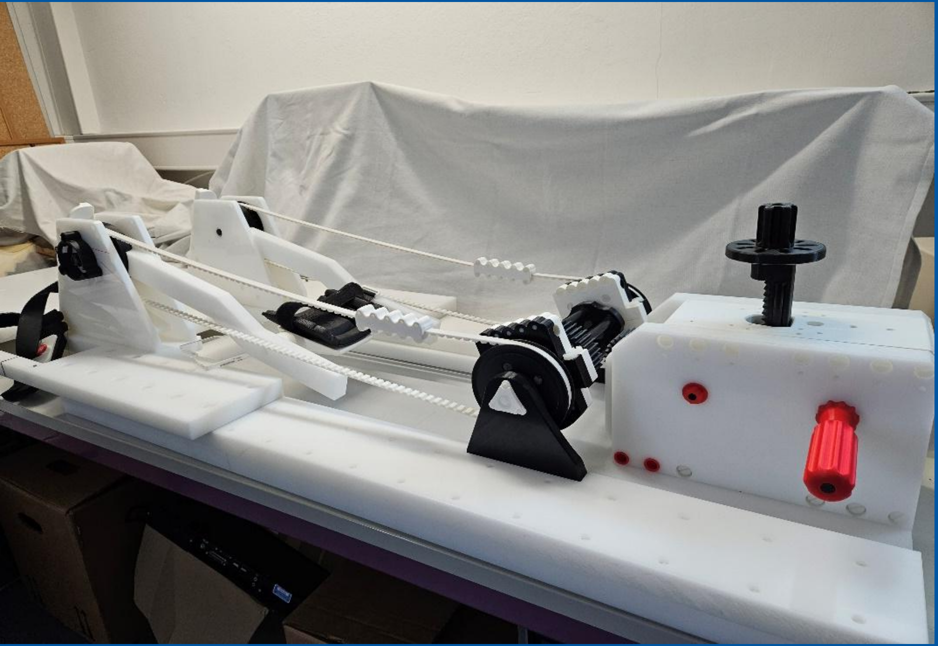

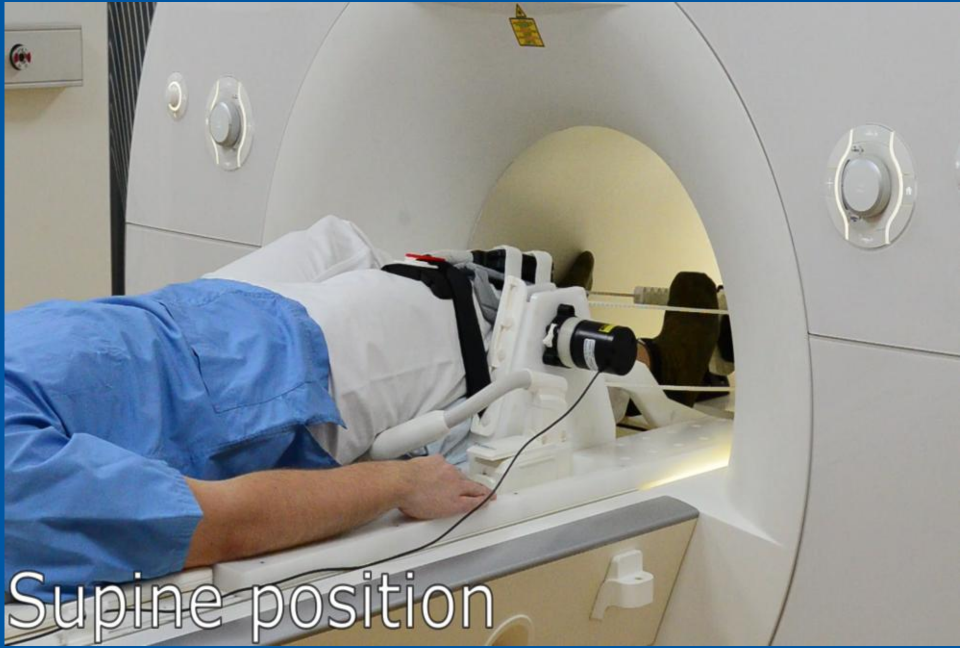

Brisson, et al. DOI:10.1016/j.zemedi.2021.12.002

MRI-compatible knee motion device

MRI-Compatible Motion Device

- Custom-designed device for controlled knee movement during MRI
- Allows for cyclic flexion-extension at consistent rates
- Integrated position sensor captures knee angle data

Dynamic CINE MRI

- Series of images showing knee joint motion during flexion-extension
- Reconstructed by sorting k-space data into discrete knee angle intervals
- Enables visualization of in vivo knee movement

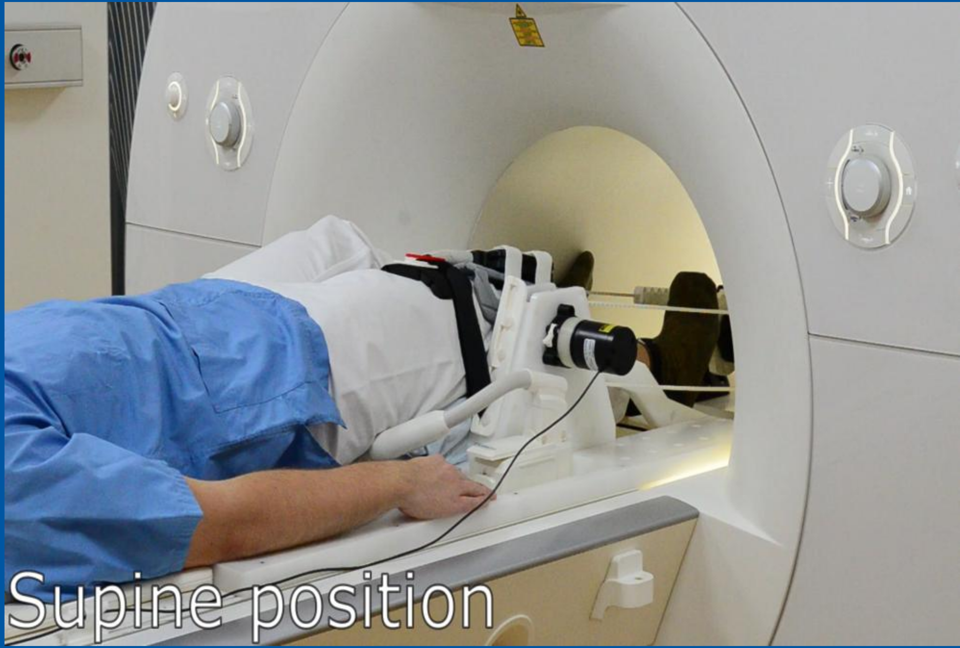

Brisson, et al. DOI:10.1016/j.zemedi.2021.12.002

Image Acquisition and Reconstruction

Participants:
- Five healthy volunteers (24-39 years)
- Controlled knee flexion-extension with metronome (7.5 cycles/min)

MRI Parameters:
- 3T scanner, 2D radial golden-angle FLASH
- TE/TR = 2.51/5.8 ms, flip angle 8°
- 176 × 176 matrix

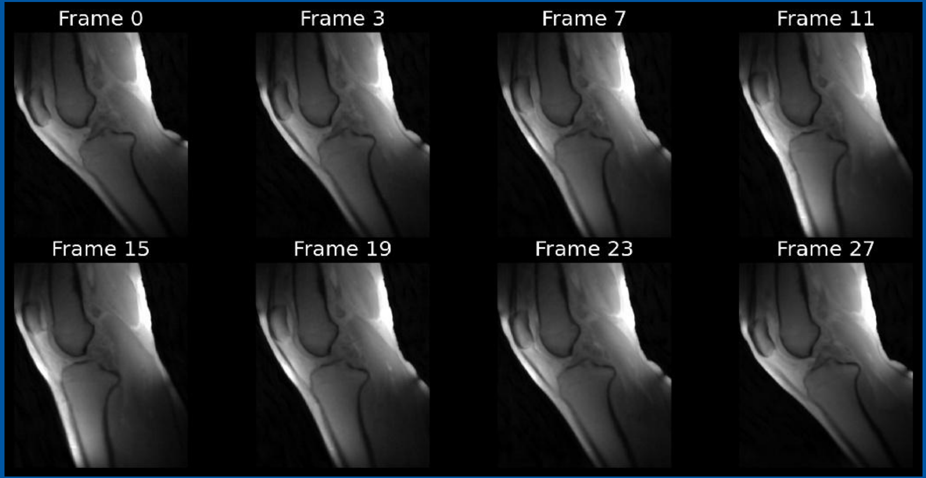

Reconstruction
- K-space data sorted into 2° knee angle windows using optical sensor data
- Each CINE frame represents a specific knee angle position

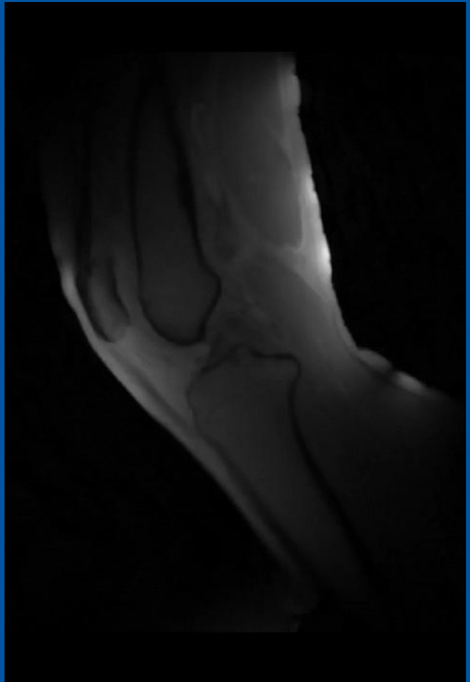

Aleksiev, et al.
DOI: 10.1016/j.mri.2022.06.015

Approach

- A combination of edge detection with connected-component labeling and frame-to-frame transformation optimization
- Used to track bone boundaries during knee flexion-extension cycles during dynamic MRI
- Four-step pipeline for continuous bone tracking across motion frames
- Method validated in five healthy volunteers and compared with manual segmentation

Bone Tracking Algorithm

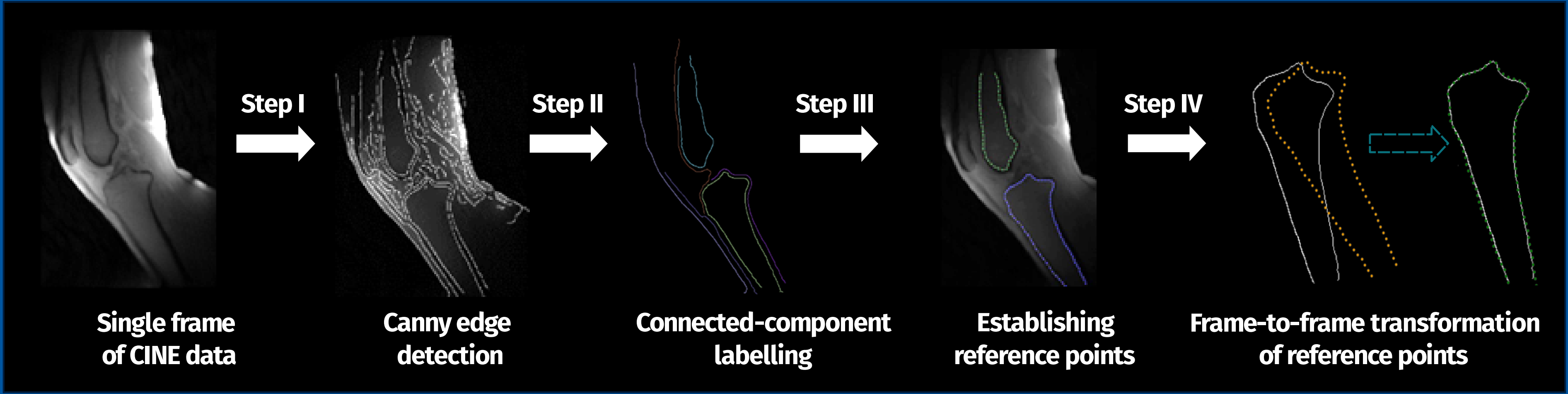

Algorithm assumptions:

- Rigid body motion in 2D sagittal plane
- Three transformation parameters: two translations, one rotation

Segmentation and Kinematic Measurement

Semi-Automated Segmentation:

- Manual bone segmentation in first frame only
- Algorithm propagates segmentation to all subsequent frames

Kinematic Measurement:

- Calculated bone segment centroids
- Measured tibia-to-femur centroid displacement per frame
- Data expressed as motion cycle percentage

Validation:

- Manual segmentation of all frames for comparison
- Boundary alignment error: average distance between transformed points and detected edges
- Inter-subject displacement variability measured

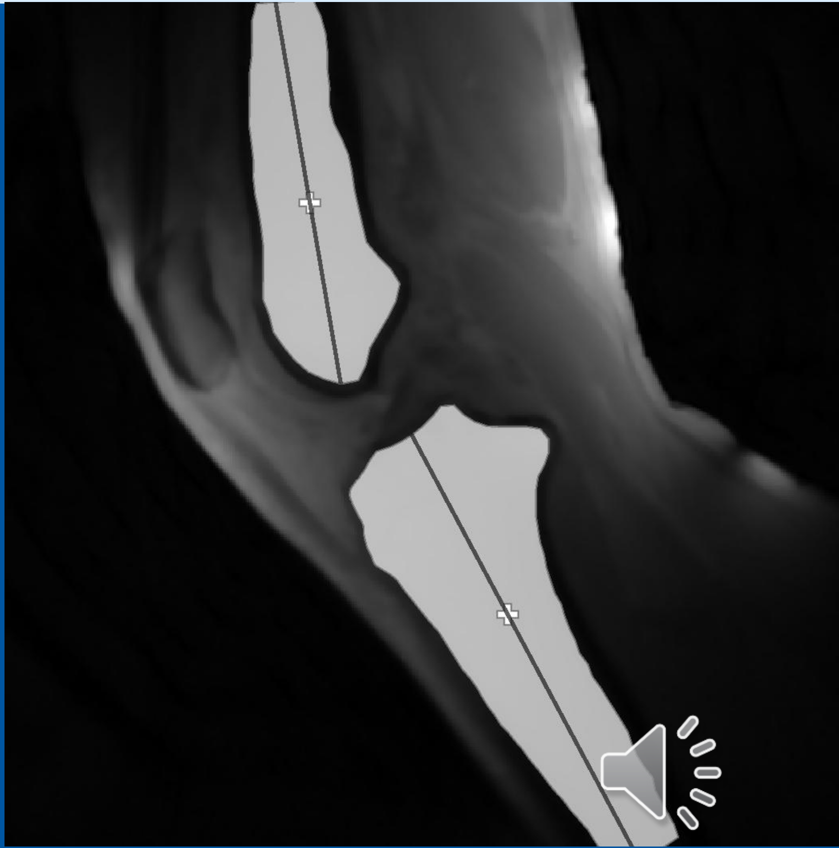

Results

- Successful tracking of both tibial and femoral bone edges throughout the motion cycle
- Alignment error: 0.40 ± 0.02 mm for both bones
- Processing time: <5 minutes (semi-automated) vs. ~15 minutes (manual)
- Horizontal displacement: 8-28 mm with linear trend during motion cycle
- Vertical displacement: Relatively constant at ~57 mm
- Improved measurement precision with smaller standard deviations compared to manual approach

UNIVERSITÄTSKLINIKUM jena

Bone Tracking Visualization

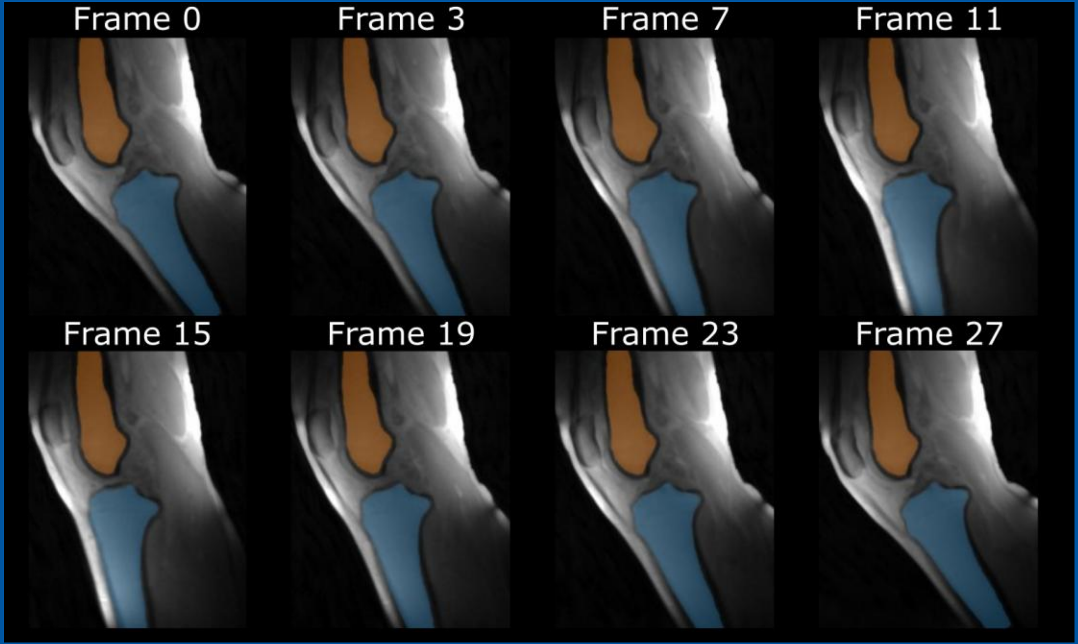

Results and Discussion: Relative Bone Displacement

Quantitative Results

- **Alignment Error**: 0.40 ± 0.02 mm (average for both bones)
- **Processing Time**: <5 minutes (semi-automated) vs. ~15 minutes (manual)
- **Horizontal Displacement**: 8-28 mm (linear trend during motion cycle)
- **Vertical Displacement**: Relatively constant at ~57 mm

Measurement Precision

- **Horizontal Displacement SDs**:
    - Semi-automated: 1.7–2.7 mm
    - Manual: 2.2–3.3 mm
- **Vertical Displacement SDs**:
    - Semi-automated: 0.7–1.2 mm
    - Manual: 0.9–1.7 mm

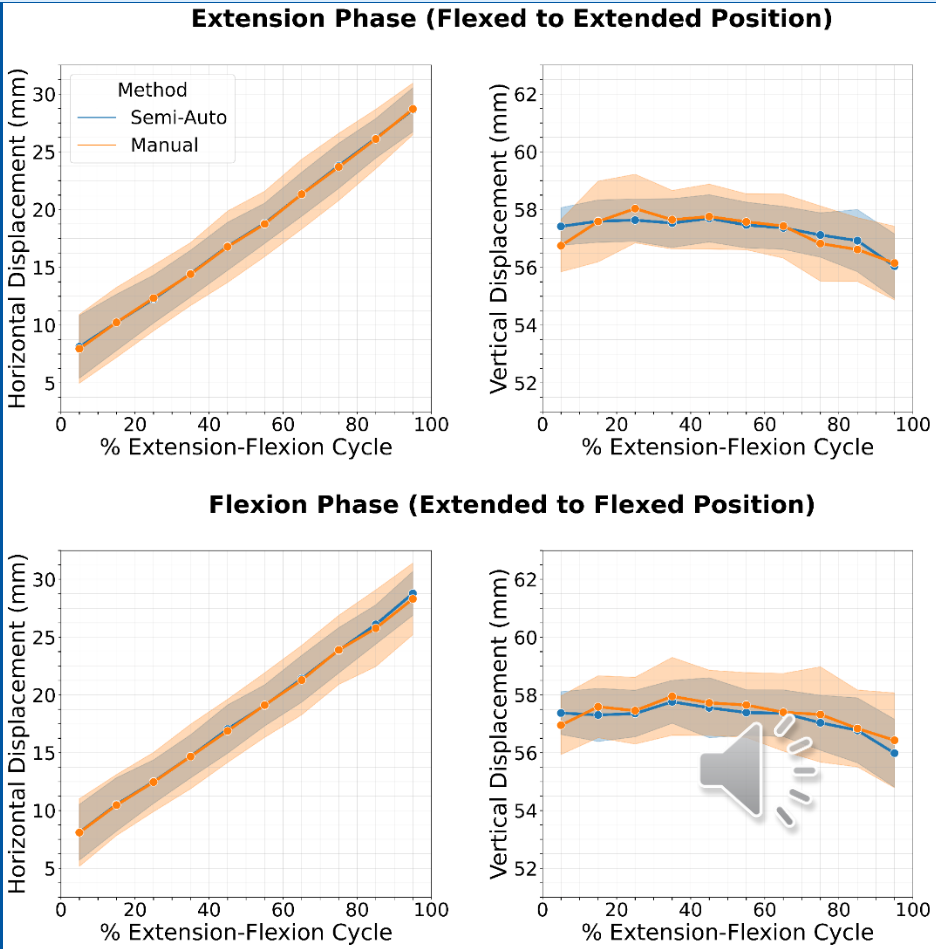

UNIVERSITÄTSKLINIKUM jena

Results and Discussion: Relative Bone Displacement

Key Findings

- Semi-automated method shows consistently lower variability
- Both methods capture similar motion patterns
- Semi-automated tracking provides more consistent measurements
- 67% reduction in processing time per dataset

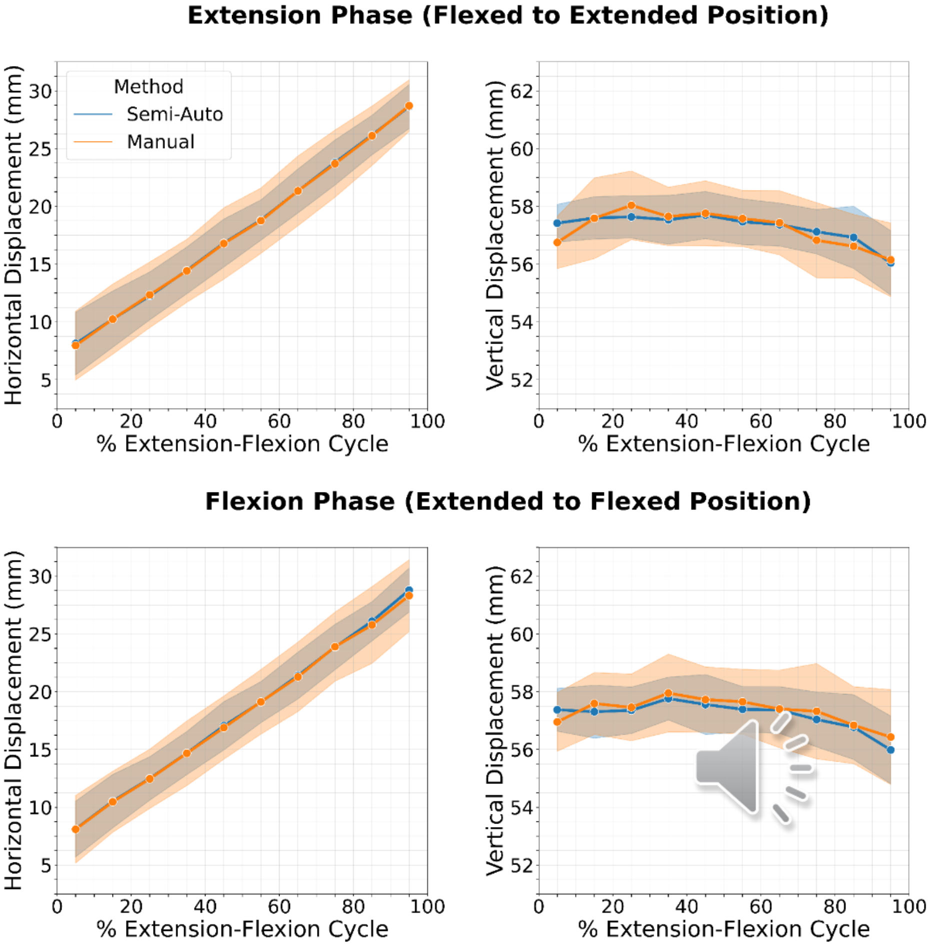

Impact and Conclusion

Technical Advantages

- Works directly on dynamic MRI without reference scans
- Uses complete bone contour for robust tracking versus landmark methods
- Maintains precision while reducing processing time
- Simplifies workflow for faster acquisition and analysis

Clinical & Research Value

- Enables study of abnormal knee mechanics
- Applicable for pathological kinematics analysis
- Allows efficient joint function monitoring
- Supports larger studies through reduced processing time

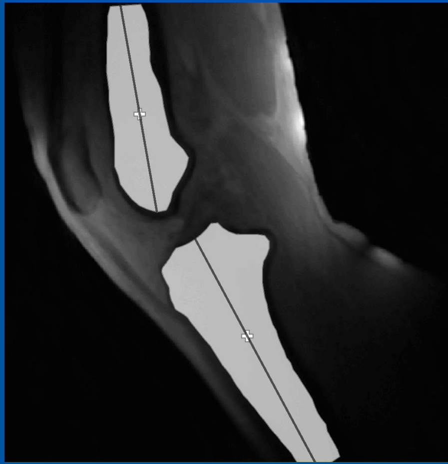

Conclusion

- Novel semi-automated tracking method validated for 2D sagittal CINE MRI
- Achieved 0.40 ± 0.02 mm alignment error with 67% faster processing
- Improved consistency with smaller standard deviations
- Suitable for both research and potential clinical applications

Acknowledgment

This work was supported by the German Research Foundation (Deutsche Forschungsgemeinschaft; KR 4783/2-1, BR 6698/1-1).

Gefördert durch

DFG Deutsche Forschungsgemeinschaft